LA-UR -82-1749

Conf-820822--2

NOTICE

PORTIONS OF THIS REPORT ARE ILLEGIBLE.

It has been reproduced from the best available copy to permit the broadest possible availability.

Los Alamos National Laboratory is operated by the University of California for the United States Department of Energy under contract W-7405-ENG-36.

MASTER

LA-UR--82-1749

DE82 018452

TITLE: IMAGE SHUTTERS: GATED PROXIMITY-FOCUSED MICROCHANNEL-PLATE (MCP) WAFER TUBES VS GATED SILICON INTENSIFIED TARGET (SIT) VIDICONS

AUTHOR(S): G. J. Yates, N. S. P. King, S. A. Jaramillo, J. W. Ogle, B. W. Noel, and N. N. Thayer

SUBMITTED TO: Society of Photo-Optical Instrumentation Engineers (SPIE) Conference, San Diego, CA, August 21-27, 1982

Los Alamos National Laboratory
Los Alamos, New Mexico 87545

FORM NO 836 R4
ST NO 2629 6/81

348-37

Image shutters: Gated proximity-focused microchannel-plate (MCP) wafer tubes vs gated silicon intensified target (SIT) vidicons

G. J. Yates, N. S. P. King, S. A. Jaramillo, J. W. Ogle, B. W. Noel

Physics and Design Engineering Divisions, Univ. of Calif., Los Alamos National Laboratory
P. O. Box 1663, Los Alamos, New Mexico 87545

N. N. Thayer

Science Department, EG&G Inc., Los Alamos Operations
P. O. Box 809, Los Alamos, New Mexico 87544

Abstract

The imaging characteristics of two fast image shutters used for recording the spatial and temporal evolution of transient optical events in the nanosecond range have been studied. Emphasis is on the comparative performances of each shutter type under similar conditions. Response data, including gating speed, gain, dynamic range, shuttering efficiency, and resolution for 18 and 25-mm-diam proximity-focused microchannel-plate (MCP) intensifiers are compared with similar data for a prototype electrostatically-focused 25-mm-diam gated silicon-intensified-target (SIT) vidicon currently under development for Los Alamos National Laboratory.

Several key parameters critical to optical gating speed have been varied in both tube types in order to determine the optimum performance attainable from each design. These include conductive substrate material and thickness used to reduce photocathode resistivity, spacing between gating electrodes to minimize inter-electrode capacitance, the use of conductive grids on the photocathode substrate to permit rapid propagation of the electrical gate pulse to all areas of the photocathode, and different package geometries to provide a more effective interface with external biasing and gating circuitry.

For comparable spatial resolution, most 18-mm-diam MCPs require gate times > 2.5 ns while the fastest SIT has demonstrated sub-nanosecond optical gates as short as ∿ 400 ± 50 ps for full shuttering of the 25-mm-diam input window.

Introduction

High-speed framing cameras are a basic diagnostic tool for recording short-lived transient optical events. Currently, we routinely use a gatable proximity-focused microchannel-plate (MCP) intensifier coupled fiber-optically to a focus-projection, scan (FPS)[1] vidicon for image shuttering and frame storage. An FPS vidicon with electrostatic deflection was selected for TV readout because of its high-resolution electron optics and fast readout capabilities. Our recent studies[2,3] of the optical gating properties of 18-mm-diam MCPs (ITT F4-111) have shown limitations in shuttering speed and image focusing for gate times shorter than ∿ 2.5 ns. The reduced response at short gate times is attributed to slow build-up of the electric field across the gated interface caused by the high capacitance and the relatively high resistivity of the photocathode-to-channel-plate interface. The proximity-focusing design used in these intensifiers restricts the photocathode-to-microchannel-plate space to ∿ 5.0 to 10.0 mils (0.127 to 0.254 mm) thereby producing a high capacity interface, which is difficult to charge quickly, resulting in slowed gate response.

We have developed a gatable silicon-intensified-target (SIT) FPS vidicon with low gate-interface capacity by using a high-conductivity gating grid spaced ∿ 50 mils (1.27 mm) from the photocathode. The photocathode is deposited on a segmented low-resistivity nickel substrate which can be simultaneously and symetrically driven from four 90°-spaced inputs that are aligned with the legs of a conductive aluminum oxide cross hair used to divide the photocathode into four quadrants.

In addition, the SIT-FPS tube, G.E. E7821G, provides higher resolution than an equivalent area MCP-FPS combination. The increased resolution results from the superior electron optic coupling used in the SIT because the photocathode and the vidicon target are in the same envelope. For the MCP-vidicon combination, the external fiber-optic couplers required between the MCP phosphor and the vidicon target cause resolution losses as well as the poorer resolution associated with the proximity-focusing mechanism itself. In effect, the E7821G is designed to replace two tubes, a gated image intensifier tube and a TV camera tube.

348-37

The characterization systems

The primary system shown in Fig. 1 uses a mode-locked dye laser with a triggerable cavity dumper followed by a Pockels cell to provide a rate-selectable train of ∿ 6 ps FWHM 650 nm light pulses with ∿ 20 ps jitter. This allows the examination of image shutter optical behavior during different times throughout the shuttering sequence. The dual Pockels cell and cavity dumper arrangement provides better rejection of unwanted laser pulses.

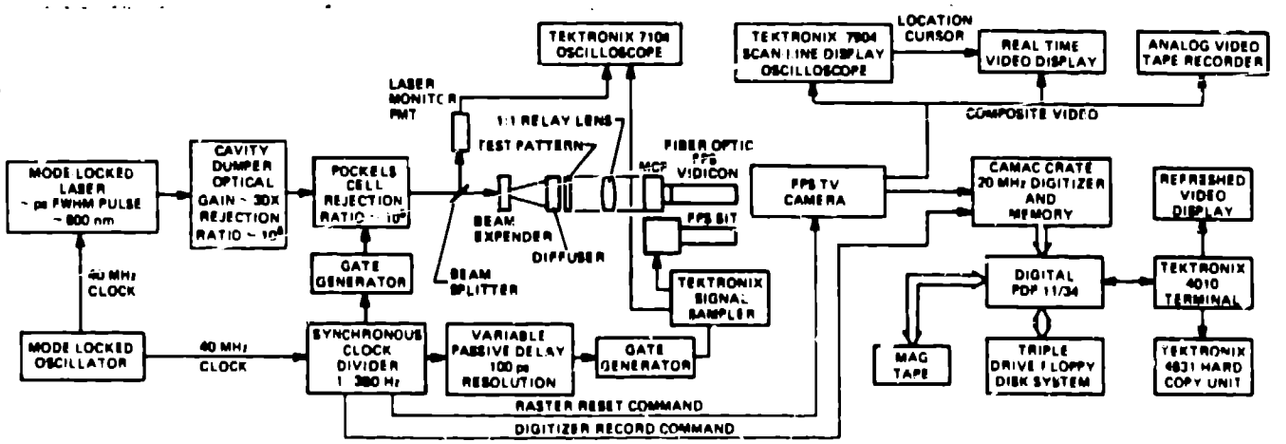

Figure 1. The primary characterization system.

The argon-ion laser mode-locked system is driven by a 40-MHz sine wave which also drives a synchronous counter to provide reduced frequencies in range of 1 to 360 pps. These are then fanned out by a four-way signal splitter. One leg triggers the laser cavity dumper and the Pockels cell which transmit one 6-ps pulse. The second leg triggers the gate generator which drives the image shutter. The third leg resets the scan on an FPS TV camera which is used either (1) to house the gated SIT under test or (2) to scan the phosphor of the MCP (which is fiber-optically coupled to an internal vidicon) under test. The fourth leg synchronizes a high-speed video digitizer to record a single TV field for each laser pulse.

The relative delay between the laser and the electrical gate pulse is varied and the gated image is stored by recording the FPS TV camera's video output with the digitizer. The relative timing between the MCP gate and the optical sampling pulse is accomplished using the variable-passive-delay unit. With this unit the laser-to-electrical gate relative timing has a range of 99.9 ns in 0.01-ns steps. In this way, the total shutter sequence is measured, giving the optical gate width for the image shutter under test. The data field is then transferred to a PDP-11/34-controlled display system for analysis. Selected data fields are rewritten on 9-track magnetic tape for later processing.

On-line analysis of the video is provided by an oscilloscope and a Hewlett-Packard 1311 XY display. A Tektronix 7104 oscilloscope is used to monitor the electrical gate through a signal sampler for purposes of aligning the optical gate with the laser pulse. This scope is also used to monitor the laser pulse intensity via a MCP-PMT viewing the laser beam through a beam splitter. The primary light pulse is expanded by a divergent lens and diffused. The diffuser is necessary to minimize interference effects from the coherent light source. For focusing and resolution measurements, a standard Air Force resolution pattern is placed on the back side of the diffuser and a relay lens is used to image the pattern onto the photocathode of the shutter tube. For other studies this pattern is replaced by an iris for controlling the illuminated area.

A second light system uses a pulsed laser diode (Hamamatsu Model HTV-C1308) that provides pulses of ∿ 100 ps FWHM at 820 nm. Synchronizing and phasing of the light and electrical gate pulses is accomplished in the fashion described for the primary system. This triggerable light source is used primarily for measurements where integration of the 40 MHz laser pulse train (although gated via both the cavity dumper and the Pockels cell) produces leakage signal strengths sufficiently large to interfere with the signal strength from the gated pulse.

The image shutters

Cross sections of the MCP and the SIT are shown in Figs. 2 and 3. Image section details for both tubes and the calculated capacitances for various sections of each gated interface

348-37

are included to emphasize basic differences between the proximity and pinhole-focused designs.

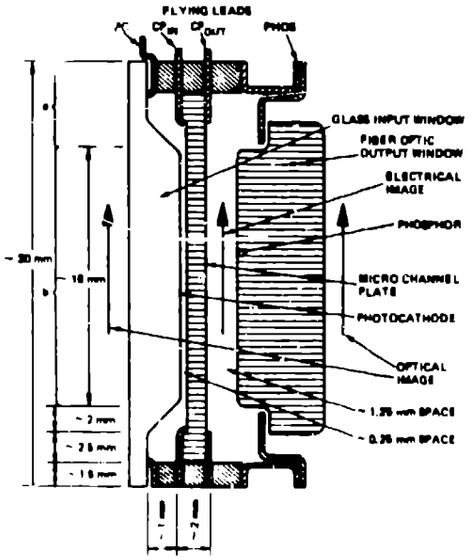

Figure 2. Idealized functional diagram for the 18-mm-diam MCP. The perimeter capacitance (section a) is ∿ 20 pfd and the gate interface capacitance (section b) is ∿ 10 pfd. For 25-mm-diam MCPs, the capacitances for a and b are ∿ 50 pfd and 25 pfd respectively.

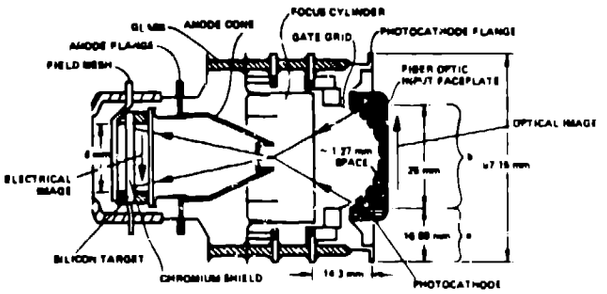

Figure 3. Idealized functional diagram for the 25-mm-diam SIT. The perimeter capacitance (section a) is ∿ 7.5 pfd and the gate interface capacitance (section b) is ∿ 3.5 pfd.

Figure 4 shows the single envelope SIT-FPS, GE Z7821G at the bottom and the two envelope MCP-FPS, ITT F4-111 and GE Z7803 fiber optic vidicon at the top. A close-up of the conductive cross hair SIT is in Fig. 5.

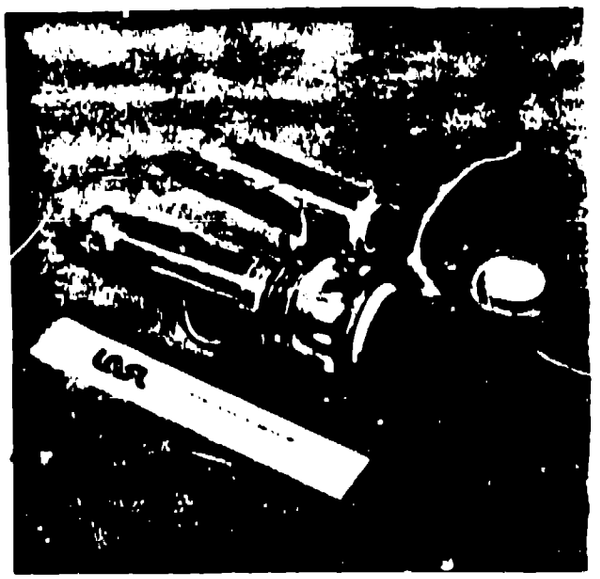

Figure 4. The SIT-FPS (bottom) and the MCP-FPS (top) are shown with 6-inch scale.

Figure 5. The segmented SIT with photocathode conductive cross hair. Each leg (center-to-edge) is ∿ 6 M.

348-37

Measurements

Gating speed

An ideal image shutter should provide uniform gain and resolution over the entire gated input photo surface with response times fast enough to produce optical gates which exactly follow the driving electrical gates. If this were the case, good correlation between the two gates would eliminate the requirement for individually testing each unit. Unfortunately, these conditions are not completely met by either image shutter at the shortest gate times, although the best SITs appear to correlate fairly well down to ∿ 400 ps.

Two dominant turn on, turn off patterns for the shutter sequence (shown in Fig. 6) were observed for MCPs with most units favoring the "normal" pattern. Some MCPs exhibit both patterns, depending upon the magnitude of the forward-biasing gate pulse. However, when over-driven, those MCPs usually exhibit the "normal" pattern. A typical complete shutter sequence for the slower SITs including turn on, fully on, and turn off phases is similar to the "abnormal" pattern for the MCPs. This sequence is the dominant sequence for SITs. In this sequence, optical turn on starts at the perimeter and propagates inward, producing a diminishing-iris effect until full turn on is achieved. The turn off phase starts at the center and propagates outward with increasing-iris effect until the tube is completely off again. The last portion (central region of the photocathode) to finish turning on is also the first portion to begin turning off. This represents the faster gate function (for either image shutter type) for optimum gating speed for the central region of the photocathode. The "normal" sequence for MCPs is characterized by a similar turn on phase but the turn off starts at the perimeter and propagates inward with the center region turning off last. This type of sequence is rarely seen in SITs. The fastest SITs show no iris pattern during the shutter sequence. Instead, the photocathode appears to transmit nearly simultaneously over the full area with increasing gate time or gate amplitude giving increased gain. See Fig. 6 for the iris-free shutter sequence.

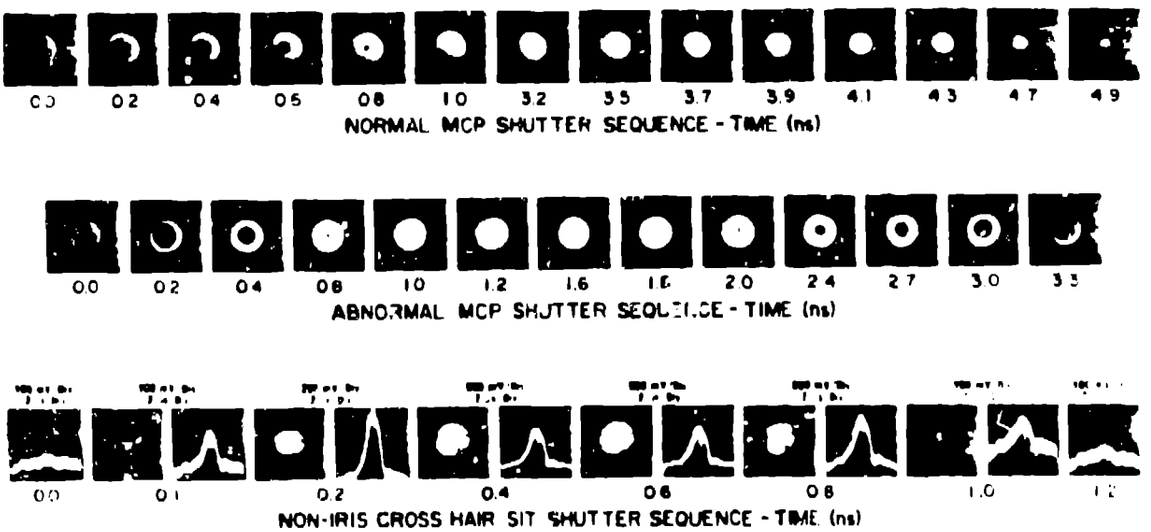

Figure 6. Observed shutter sequences. Zero time indicates beginning of the optical gate.

Good correlation between the measured gating speed and the calculated gate interface RC time constant was seen with the fastest tubes for both types. The shortest RC time constants had the fastest shutter times. The two close-spaced SITs with photocathode-to-gate grid spacing = 25 mils (0.635 mm) and with no photocathode conductive underlayer measured optical gate times of 4.2 and 5.8 ns respectively. The medium-spaced SITs with gate spacing = 50 mils (1.27 mm) and with nickel substrates achieved shuttering over the total 491 mm^2 in ∿ 1.0 to 1.5 ns. Both 25-mm-diam MCPs with gate interface capacitances ∿ 25 pfd and with single-undercoated photocathodes gated the slowest measuring ∿ 6 to 7 ns.

The optical gating tests were repeated, restricting the image area to ∿ 254 mm^2 (∿ 18-mm-diam circle) in the center of the SIT photocathode. This was done to compare the SIT performance over the reduced area with typical gating speeds observed earlier by us with 18-mm-diam MCPs. Our results indicated that most 18-mm-diam MCPs must be gated for fully on (total area transmitting) times ∿ 2.5 ns in order for the proximity-focusing field to develop sufficiently to give good focus in the center of the tube. The two fastest 18-mm-diam MCPs, one with single undercoating (SN 788/7) and one with double undercoating (SN 788/10) gated in 1.2 and

348-37

1.5 ns respectively, although with reduced center resolution. The faster non-crossed SITs gate with good focus over their central 18-mm-diam in ∿ 600 to 900 ps and the slower SITs gate in ∿ 2.5 ns.

Two F4-111 MCPs were modified to increase their potential for fast gating. One unit was fabricated with 9-mm-diam active photocathode and the other with increased gate spacing (∿ 20 mils). These modifications reduced area and capacitance of the actual photocathode-to-MCP interface. Unfortunately, other critical parameters were not controlled with the result that both units gated much slower (∿ 5 ns) than expected.

The SIT with a conductive photocathode cross hair was gated in ∿ 400 ps when multipoint driven with an ∿ 400 ps FWHM current pulse from a synchronized (with the laser) linear electron accelerator (LINAC) - Faraday Cup detector.

The optical shutter times for one of the slowest SITs, one of the fastest non-crossed SITs, the cross hair SIT, and two randomly-selected 25-mm-diam MCPs are plotted in Fig. 7. The shutter sequence for the cross hair SIT is shown in Fig. 8.

The response time (time between the leading edge of the electrical gate pulse at the image shutter input leads and the start of optical transmission through the shutter) is ∿ 2.0 ns for most MCPs and ∿ 1.5 ns for most SITs. The delay for the MCPs is not clearly understood. The SIT delay is associated with the transit time (0.91 to 1.70 ns) spread through the image section.

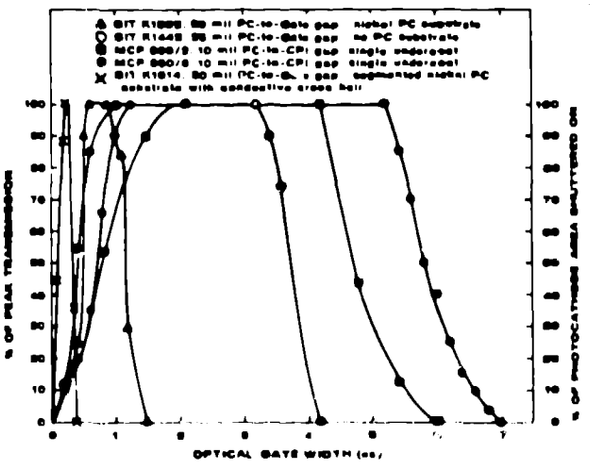

Figure 7. Optical gates for three 25-mm-diam SITs and two 25-mm-diam MCPs. The internal transit times for all units have been normalized to zero. The left-hand ordinate is for SIT K1614 and the right-hand ordinate is for the remaining tubes.

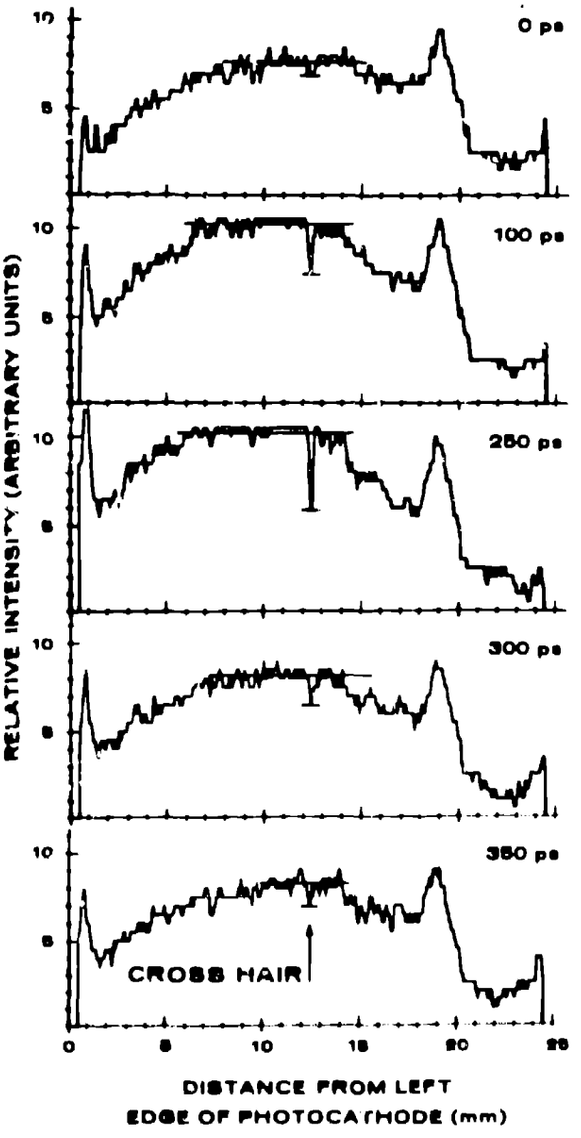

Figure 8. The shutter sequence for SIT SN K1614 with a segmented photocathode. These intensity profiles were taken with all four legs of the cross hair simultaneously driven with ∿ 60 V ∿ 400 ps FWHM gate pulse. The opaque cross hair is seen as the negative spike in the center of the profiles. This SIT showed no iris effect during the shuttering sequence. The poor signal-to-noise ratio for these data resulted from integration of the insufficiently reduced 40 MHz laser pulse train. The Pockels cell which reduces the gated pulses by ∿ 50% and the non-gated pulses by ∿ 10^3 had been removed for other tests and was not in place when these data were taken.

348-37

These tests show ∿ 3.33 X faster response for the central 18-mm-diam of the SIT than for the total 18-mm-diam for the MCPs. The comparison between units of equal input area show even greater advantages, up to ∿ 5X, for the SIT. The gating speed of MCPs should also increase with the use of the conductive cross. This is being explored with the MCP manufacturer. At present however, the crossed SIT can be expected to gate > 10X faster than their 25-mm-diam MCP counterparts and > 5X faster than the 18-mm-diam MCPs.

Resolution

The resolution tests were done using the same setup as for the gating-speed tests with a standard Air Force resolution pattern as an image. The pattern was first imaged at the center of the photocathode. After viewing the entire pattern to look for large-area uniform focus, the TV camera raster was reduced to scan only the area on the photocathode where the higher spatial frequencies were imaged. The zoom in no way changes the image frequency or otherwise compromises the resolution tests, but rather, it simply allows us to view the area of interest with higher time and spatial resolution. These tests were performed using the ∿ 6 ps FWHM laser pulse with sufficient intensity to operate the silicon target just below saturation with a single laser pulse. This was done to provide an extreme case of electron density in the crossover region of the SIT to investigate predicted resolution losses from space charge defocusing.

One set of resolution data for two 25-mm-diam tubes (SIT SN K1602 and MCP SN 886/2) was taken in the following three steps: (1) in the DC mode where the tube is statically biased to the continuously shuttered-on condition, (2) in the gated mode where the tube is shuttered on for the shortest gate time consistent with a selected resolution requirement and (3) in the AC or gated mode where the tube is quiescently biased off, then is shuttered on for the shortest achievable gate time for full area photocathode transmission independent of resolution criteria. For both tube types, losses in CTF (Contrast-Transfer-Function) were noted when comparing the static resolution with the resolution for various optical gate widths. The video images and the scan-line intensity profiles for these tests are found in Figs. 9 and 10. Inspection of these figures shows much better resolution in all cases for the SIT. In fact, the resolution obtained from the SIT when gated for ∿ 2.5 ns is superior to that obtained from the MCP in the DC mode, and the SIT resolution at ∿ 1.5 ns is comparable to the MCP DC resolution. The measured CTF at 4.5 and 8 lp/mm for the SIT were 70 and 67% at DC, 60 and 30% at 2.5 ns, and 56 and 10% at 1.5 ns. For the MCP, these were 48 and 15% at DC, 36 and 11% at 6.0 ns. For the 4.0 ns gate, the MCP could not resolve either set. These tests indicate that the present gated SIT design is capable of providing spatial resolution of better than 10 lp/mm with the 6 ps FWHM light pulse in either the DC or gated modes with the limiting resolution in DC > 20 lp/mm. Because the SIT is intended to provide nominal optical gates of ≥ 1 ns with anticipated absolute minimum gates of ∿ 400 ps ± 100 ps, the laser pulse represents an approximate 15 to 50X worse-case (over the design-goal case) for charge density.

Two additional resolution-related distortions have been observed, one for each tube type. The SITs, like most electrostatically-focused image tubes show "pin-cushion" distortion. The cause is related to the dependency of image magnification on the distance of the image plane from the electron lens axis which is variable because of the flat target. The magnitude of this problem has not been quantified. However, the distortion appears about equal for the DC and gated modes so geometric restortation can be applied to the data during processing.

The MCPs, when gated for short times have poorer resolution in the center region than near the edge. This is caused by the spread in the magnitude of the transient proximity-focusing voltage which immediately after application, is strongest near the edge of the MCP. Therefore, the edge region of the gated interface has sufficient electric field to accomplish satisfactory focusing while the center has insufficient field, resulting in the unfocused condition depicted in Fig. 11. At longer gate times, the proximity-focusing fields are established over the entire gated interface and the center and edge resolution are nearly equal.

The conductive cross hair SIT resolution was measured at optical gate width ∿ 700 ps ± 100 ps. The SIT was driven from one of the four gate inputs for this test. The gated optical image and the electrical gate are shown in Figs. 12 and 13.

Gain and dynamic range

For the SITs, the possibility of restricted dynamic range because of signal-induced space charge in the plane between the photocathode and the gating grid and/or in the plane between the gating grid and the anode was investigated. If the signal current as a function of the effective light pulse duration (either the actual light pulse width or the optical gate width) causes sufficient space charge to retard the signal current, the observed magnitude for saturation current should vary with pulse duration if sufficient radiant power is

348-37

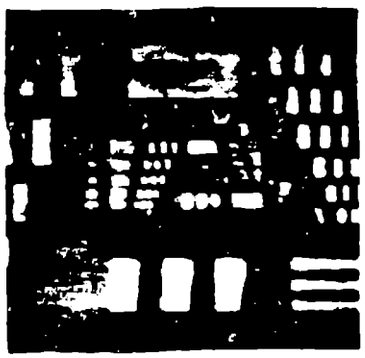

(a). MCP in the DC mode.

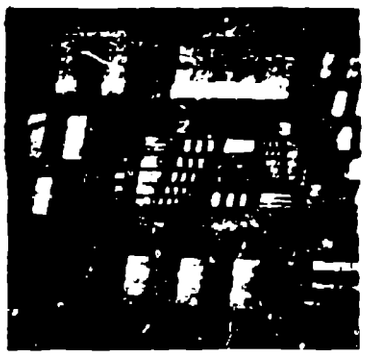

(b). SIT in the DC mode.

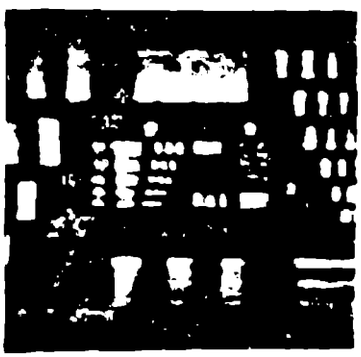

(c). MCP gated for ∿ 6.0 ns

(d). SIT gated for ∿ 2.5 ns

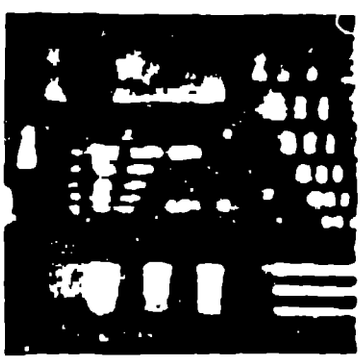

(e). MCP gated for ∿ 4.0 ns.

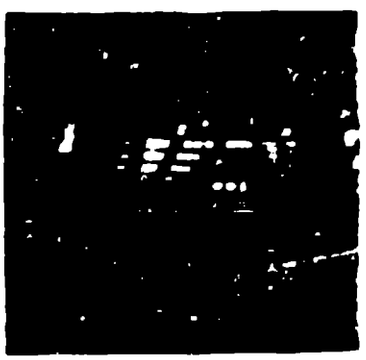

(f). SIT gated for ∿ 1.5 ns.

Figure 9. The center resolution for 25-mm-diam MCP [illegible] 866/2 and for 25-mm-diam SIT SN K1602. The contrast and peak intensity [illegible] each image has been normalized so that the resolution difference can be compared. The oval in the SIT pictures is a flaw in the electron optics of the FPS readout section. The diagonal bar pattern in the MCP pictures is not associated with the MCP.

348-37

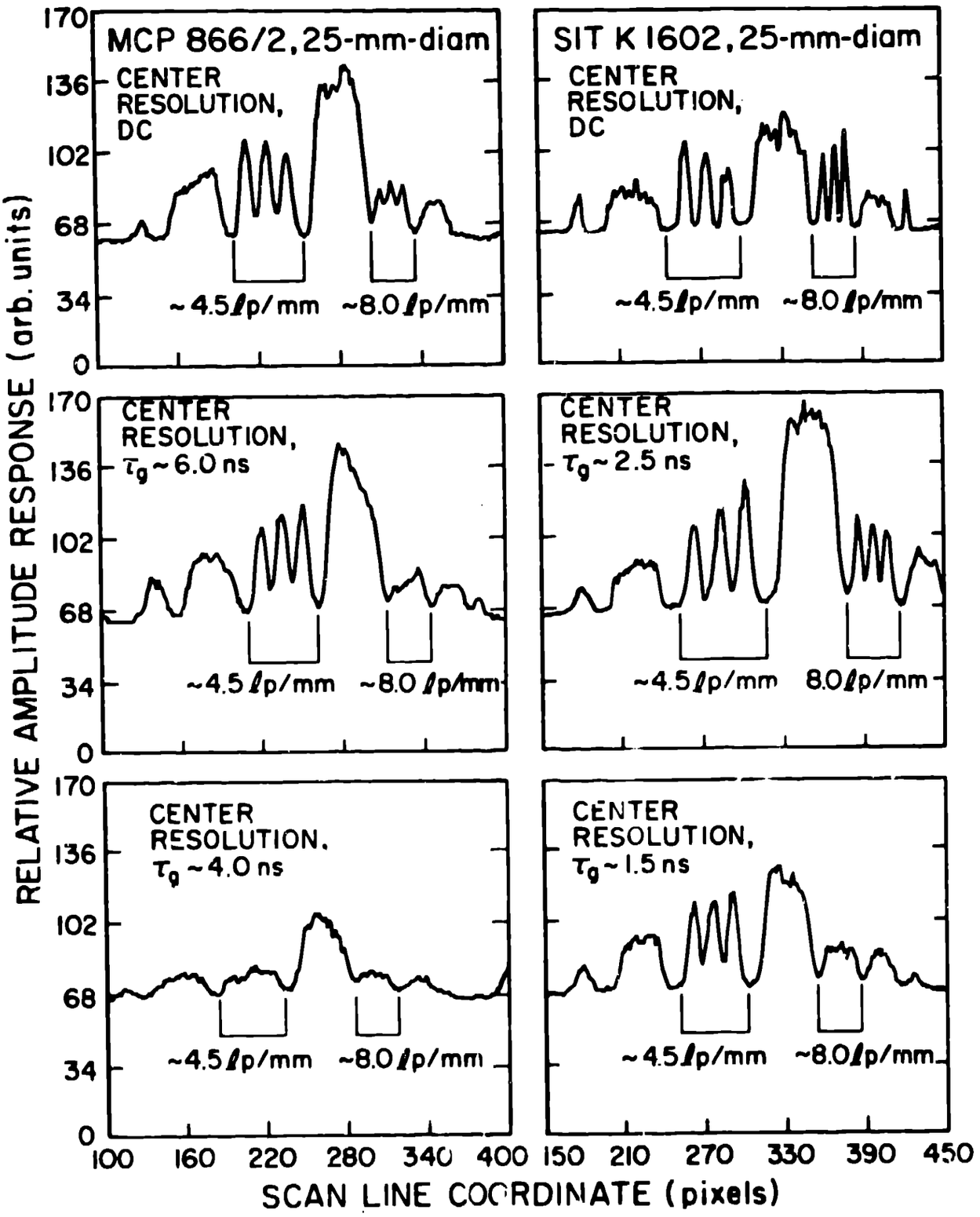

Figure 10. The scan-line profiles for estimating the CTF for the video images of Fig. 9. The input intensity for the DC measurements was attenuated to give SN similar to the gated case. For the gated data, T_g is the optical gate width.

348-37

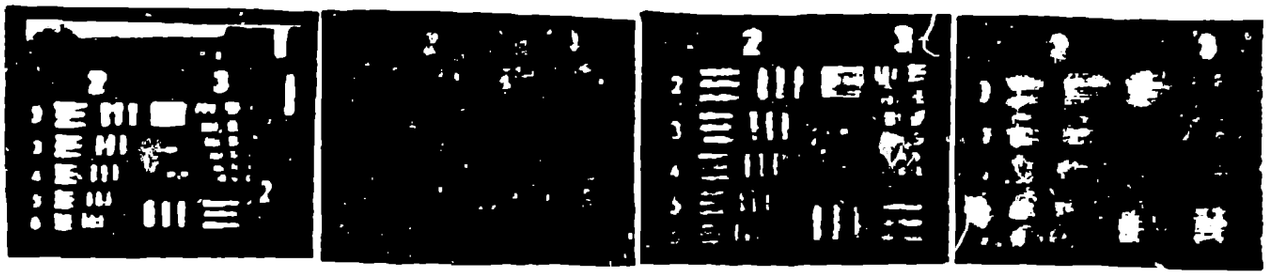

(a) Edge resolution in the DC mode. (b) Edge resolution in the gated mode for fully on time ∿ 2.5 ns. (c) Center resolution in the DC mode. (d) Center resolution in the gated mode for fully on time ∿ 2.5 ns.

Figure 11. The center-to-edge resolution for 18-mm-diam MCP SN 788/7 for the gated and non-gated modes. The pattern was first imaged near the edge and then near the center. The input intensity was attenuated for the DC measurement and all other parameters were held constant.

provided to assure saturation. Without space charge influences on current flow within the tube, the saturation observed will be due to saturation of the silicon target. This level was established first using a long-duration (∿ 3 μs FWHM) light pulse from a strobe with the SIT in the DC mode. The test was repeated with the SIT gated for 14, 6, and 1.5 ns. Next, with the SIT still gated for 1.5 ns, the 100-ps laser diode pulse was used. For all cases, the saturation current observed was ∿ 700 nA, which is consistent with our experience with nominal vidicon silicon targets. All SIT tubes tested showed no change in saturation level as a function of light pulse width in the range from 100 ps to 14 ns, although some variation in absolute level from tube to tube was noted, and significantly lower saturation was observed for the two SITs with photocathode-to-gate grid space = 25 mils (0.635 mm).

Most of these tests were performed using the iris pattern and the laser-diode source. Two SITs, two Sb_2S_3 vidicons, one silicon tgt vidicon, and one MCP were tested. The vidicons were tested individually to get their response characterized before cascading the MCP. The dynamic range measurements included the TV camera preamplifier noise. With the unit used for all our tests, the noise sets the lower limit on dynamic range. The saturating level for the SITs is set by the saturation level for silicon.

Referring to Fig. 14, the curve showing the MCP-silicon vidicon combination shows saturation at the typical silicon level. Hence, with silicon, both SITs and MCPs will have the

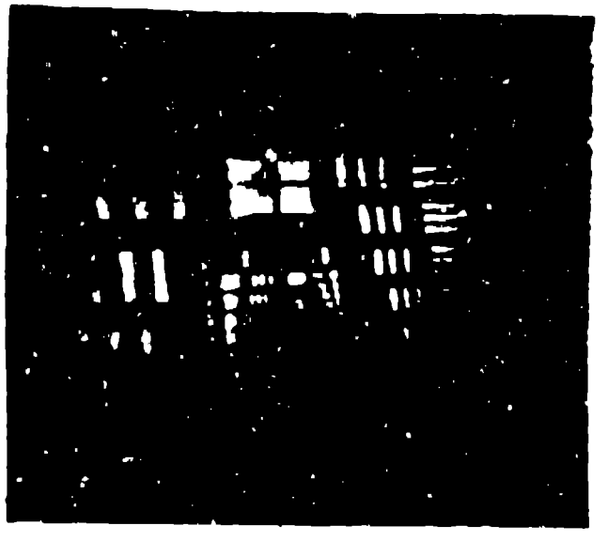

Figure 12. The cross hair SIT resolution for ∿700 ps optical gate. Note the opaque cross hair in the white portion of the recorded resolution pattern.

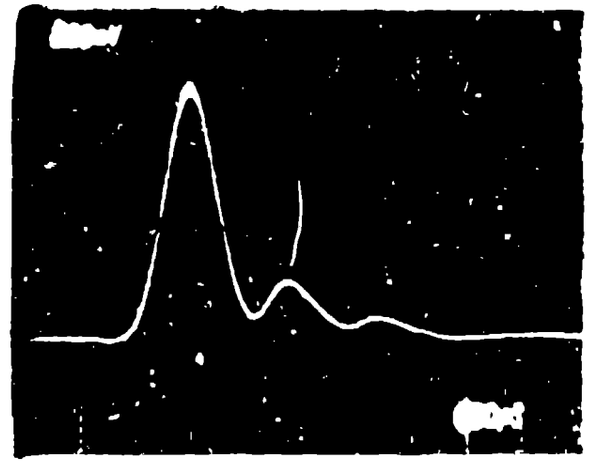

Figure 13. The electrical gate (attenuated 40 dB) for the ∿700 ps optical gate shown in Fig. 12.

348-37

same dynamic range. However, for the MCP-Sb_2S_3 combination, the MCP range can be less than or greater than that of the SIT. Under optimum conditions, the MCP outperforms the SIT in both basic responsivity (this may be partly related to different S-20 quantum efficiencies) and dynamic range. The MCP gain is ∿ 10 to 50X greater than the SIT gains measured. However, the MCP was tested at maximum gain and the SITs were tested at 25 to 50% of maximum gain. For identical photocathode responsivity, the expected difference is ∿ 10X as predicted by comparing the electron gains (∿10^3) possible from SIT targets with similar electron gains (∿10^3) possible from microchannel-plates with added luminous gain (∿10^3 between the channel-plate and the phosphor.

DC/AC gain ratios

For both SITs and MCPs, the measured gains for the shortest gated and the non-gated modes are different. The gain varies with optical gate width. The mechanisms for the increased gain in the two tube types are different.

The primary SIT gain is a function of the accelerating voltage applied between the photocathode and the anode and the chromium layer, or buffer, used on the silicon target to minimize unwanted light transmission. The chromium also serves as a barrier to photoelectron energies ≲ 3 keV. The conversion efficiency of incident photoelectrons to electron-hole charge pairs is ∿3.45 eV/pair. The SIT gain, G, is given by:

$$G = \frac{290}{(kV)} \left| V_{accelerating} - 3 \right| (kV) \qquad (1)$$

The gate grid, however, in addition to shuttering the tube also controls the gain by controlling the amount of photocathode emission that is allowed to proceed towards the silicon target. Therefore, the measured gain will also be a function of the grid bias established by the reverse bias voltage used to keep the SIT shuttered off and the magnitude of the forward-biasing gate voltage. Because the gate waveforms are essentially Gaussian, the higher amplitudes also mean wider pulses, with the result that higher gains are observed for wider optical gates. If the gate pulses had near-zero rise and fall times, increased gain with increased amplitude for no increase in gate time would probably be observed.

The MCP gain and gate controls are separate. The primary MCP gain is set by the voltage magnitude across the microchannel-plate assembly and the voltage between the channel-plate assembly and the phosphor. Our earlier study[2,3] indicated a much smaller gain function determined by the voltage across the photocathode-to-microchannel-plate space, namely the gate voltage. The response time of this gated interface is believed responsible for the observed increase in MCP gain with increasing optical gate widths.[4] The longer gates provide more time for the gate voltage to charge to a higher level, providing the increased gain.

The measured gains as a function of optical gate width for one 18-mm-diam MCP and for several SITs are found in Fig. 15 and Table 1 respectively.

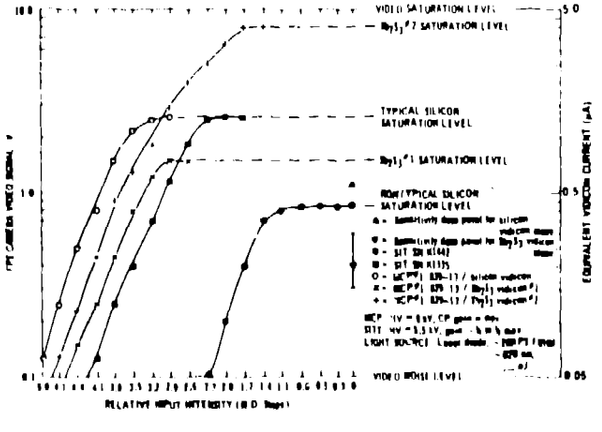

Fig. 14. The gain and dynamic range measurements.

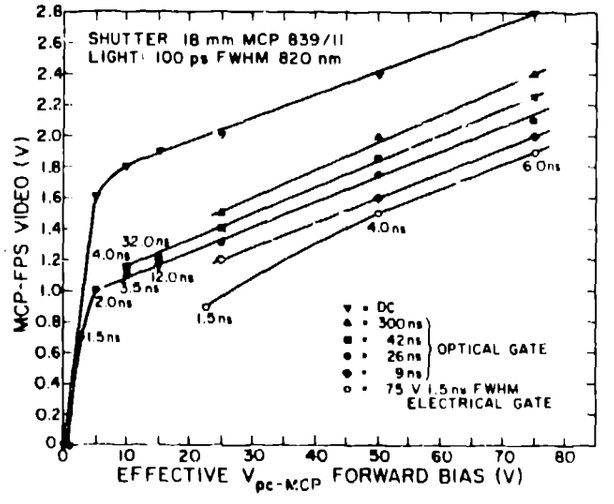

Figure 15. The gated and non-gated MCP gains as functions of optical gate width.

348-37

Shutter ratio

The ratio of the input radiant flux intensities required to give the same output signal from the image shutter when operating in the statically-on (or DC mode) condition to the shuttered off (non-gated phase of the gated mode) condition is called the shutter ratio.

For the SITs, this is a combination of (1) the retarding field strength established by the reverse-bias voltage between the photocathode and the gate grid which shutters photoelectrons, and (2) the optical feed-through which exists because of the effective pinhole camera formed by the anode aperture. Both light sources were used for these measurements. The optical feed-through which operates directly on the silicon target is wavelength dependent. The 650 nm laser emission and the 820 nm laser diode emission stimulate the target at higher quantum efficiency than the ∿ 450 ± 50 nm spectrum used in the field experiments. A low pass, narrow band optical filter will therefore improve the SIT shutter ratio.

The optical feed-through was reduced by reducing the anode entrance aperture from 6.35 mm to 2.54 mm by inserting a metallic plug with a restricting orifice in the basic cone structure. Further reductions in anode aperture were avoided to eliminate possible vignetting of the focused image beam as it goes through crossover in this region of the tube. The feed-through was also minimized by increasing the chromium layer on the silicon target reducing the nominal transmission characteristic of ∿ 20% to ∿ 2%. The optical feed-through was measured by removing the accelerating voltage from the SIT and comparing the signal with that observed in DC mode with the SIT gain functioning. For the tubes measured, the range is from ∿ 2×10^{-4} to 5×10^{-5} for optical signal feed-through.

The magnitude of reverse-bias gate voltage used depends upon the desired optic gate width. Since the bias between the photocathode and the gate grid controls the grid transmission, the shutter ratio should vary somewhat with gate width. The largest reverse biases result in the shortest optical gates. This gives the best photoelectron shutter ratios (∿ 10^3 average) for the shortest optical gates. Table 1 summarizes SIT shuttering ratios.

The shuttering efficiency (for photoelectrons) obtained for most 18-mm-diam MCPs is > 10^6 and for the better SITs is > 10^3. There is a clear advantage of ∿ 10^3 in favor of the MCP. The SIT design is being investigated to explore possible improvements, including replacing the gold-coated gate grid with a solid gold grid, deflection shuttering, etc. During processing of the photocathode, the gold-coated copper gate mesh grid reacts with the photocathode alkali materials and becomes slightly photoemissive. This is believed to be the reason for the poor shuttering efficiency. The ratio of ∿ 10^3 can be used to maximum advantage with proper attenuation of unexpected radiation, but it represents a weakness in the present SIT design.

Driving point impedance of the gate interfaces

The wide variations in observed gating speeds for typical MCP intensifiers prompted us to look for electrical parameters which could be correlated with measured optical performances. The series resistance and lumped capacitance of the MCP gate interface for several units were measured at 10 MHz with an RF impedance analyser (Hewlett-Packard 4191A) and compared with gate times measured earlier for the units. The following formula was developed [2] to predict the optical gate width, T_{gate} as a function of the gate interface RC time constant:

$$T_{gate} \sim 3.5 \times 10^{15} \, (RC)^{e-1/e} \text{ (ns)} \qquad (2)$$

Later, the complex impedance for both SITs and MCPs were measured for CW frequencies from 10 MHz to 1 GHz. These data are plotted in Fig. 16. The frequency range corresponding to our range of gate pulse widths can be approximated by calculating the capacitive reactance, X_c, of the gate interface capacity, c, to the rise time, t_r, of the gate pulse:

$$X_c = \frac{1}{2 \pi f c} \text{ , where } f = \frac{0.35}{t_r} \qquad (3)$$

This approximation is possible because our gate pulses are basically Gaussian-shaped with rise times taken between the 10% and 90% points of the FWHM of the pulse.

In the range of interest (gate widths from ∿ 400 ps to 10 ns) the SIT curves represent a purely capacitive load to external gate generators while the MCP curves indicate a frequency-dependent reactance alternating between capacitive and inductive phases. The simpler load represented by the SIT makes the design of driving circuitry much easier.

348-37

Table 1. The Shutter and Gain Ratios for Typical SITs of Several Design Versions

SIT (SN)	Shuttering Efficiency		Gain Ratio (non-gated/gated or DC/AC)			
	for Photoelectrons	for Photons	DC/AC	T_{os} (ns)	DC/AC	T_{os} (ns)
K1335	50	?	3.7	1.5	1.6	6.0
K1442	5×10^2	3.2×10^4	4.6	1.5	2.1	5.0
K1481	$8 - 12 \times 10^2$	2×10^4	3.8	1.7	2.0	5.7
K1481	$4 - 8 \times 10^2$	1×10^5	1.8	1.5	1.2	5.0
K1614	7.5×10^3	2×10^5	1.9	1.5	1.1	5.0

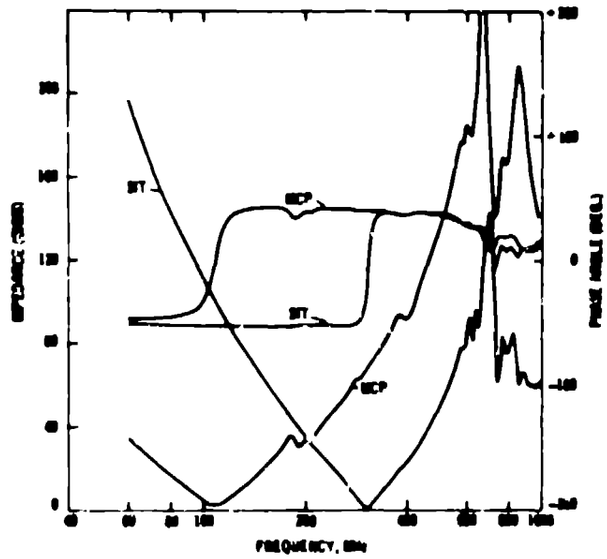

Figure 16. The impedance and phase angle plots for typical 25-mm-diam SITs and MCPs.

Acknowledgments

The authors would like to express appreciation to Mel Nelson, Chen-Hui Lin, Terry Davies, and Ian Aeby of EG&G, Santa Barbara for assistance in the design and maintenance of the measurement systems and in collecting data.

References

1) J. K. Fisher and B. H. Vine, General Electric Company, "Performance in a Small Package: The New General Electric (GE) FPS Vidicon," Proc. SPIE, Recent Advances in TV Sensors and Systems, C. F. Freeman, Ed., San Diego, CA, Aug. 27-28, 1979, pp. 2-5, Vol. 203.

2) N. S. P. King, G. J. Yates, S. A. Jaramillo, J. W. Ogle, and J. L. Detch, Jr., "Nanosecond-Gating Properties of Proximity-Focused Microchannel-Plate Image Intensifiers," Los Alamos Conf on Otpics '81, D. L. Liebenberg, Ed., Proc. SPIE 288, pp. 426-433 (1981).

3) N. S. P. King, G. J. Yates, S. A. Jaramillo, J. W. Ogle, B. W. Noel, and J. L. Detch, Jr., "Optical and Electrical Characteristics of Nanosecond-Gated Proximity-Focused MCP Image Intensifiers," Proc. 1981 IEEE Intl Conf on Plasma Science, Santa Fe., NM, May 18-20, 1981, p. 144.

4) J. L. Detch, Jr., and J. W. Ogle, "A Distributed R-C radial Transmission Line Theory Applied to the Gain Characteristics of Gated Microchannel-Plate Image Intensifiers," EG&G report EGG 1182-2404 S-699-R (June 1980).